

# IMAGE DEBLURRING COMBINING POISSON SINGULAR INTEGRAL AND TOTAL VARIATION PRIOR MODELS

Hiram Madero-Orozco<sup>1</sup>, Pablo Ruiz<sup>2</sup>, Javier Mateos<sup>2</sup>, Rafael Molina<sup>2</sup>, Aggelos K. Katsaggelos<sup>3</sup>

<sup>1</sup>Departamento de Ingeniería  
Eléctrica y Computación  
Universidad Autónoma de Ciudad Juárez,  
Chihuahua, México  
al116148@alumnos.uacj.mx

<sup>2</sup>Departamento de Ciencias  
de la Computación e I.A.  
Universidad de Granada,  
Granada, Spain  
{mataran, jmd, rms}@decsai.ugr.es

<sup>3</sup>Electrical Engineering and Computer  
Science Department  
Northwestern University  
Evanston, IL, USA  
aggk@eecs.northwestern.edu

## ABSTRACT

In this paper a new combination of image priors is introduced and applied to Bayesian image restoration. Total Variation (TV) image prior preserves edge structure while imposing smoothness on the solutions. However, it does not perform well in textured areas. To alleviate this problem we propose to combine TV with the Poisson Singular Integral (PSI) image prior, which is able to preserve image textures. The proposed method utilizes a bound for the TV image model based on the majorization-minimization principle, and performs maximum a posteriori Bayesian inference. In the experimental section the proposed approach is tested on synthetically degraded images with different levels of spatial activity and areas with different types of texture. Since the proposed method depends on a set of parameters, an analysis, about their impact on the final restorations, is carried out.

**Index Terms**— Deblurring, Bayesian image restoration, Total Variation, Poisson Singular Integral

## 1. INTRODUCTION

When we take a picture, we want a detailed representation of the scene, but very often the observed image is degraded. The degradation is usually caused by movement during the recording process or because the scene is out of focus. Image deconvolution is an important task in image processing. Its goal is to recover or estimate the original image  $\mathbf{x}$  from a blurred and noisy observation  $\mathbf{y}$ . The image degradation model is a convolution between the original image and the known blurring operator  $\mathbf{H}$ . It can be expressed as

$$\mathbf{y} = \mathbf{H}\mathbf{x} + \mathbf{n}, \quad (1)$$

where  $\mathbf{n}$  is Gaussian additive white noise with zero mean and variance  $\beta^{-1}$ .

Nowadays, different approaches try to solve this inverse problem. Methods based on Wavelets and Curvelets, capture and preserve sharp features in the image, and combined with threshold or shrinkage rules provide good results [1, 2].

Models based on the Bayesian paradigm provide solution to problems like blind deconvolution [3], space-variant deblurring [4], camera shake [5] and light field sensing [6]. Many of the proposed methods utilize a Total Variation (TV) image prior [7].

This research was supported by CONACYT, the Spanish Ministry of Economy and Competitiveness under project TIN2010-15137, the European Regional Development Fund (FEDER), the University of Granada under CEI Biotic project CEI2013-MP-14 and, in part by the US Department of Energy grant DE-NA0000457.

Total Variation preserves object boundaries (edges) but often eliminates image texture, because TV restricts the space of solutions to the space  $BV(R^2)$  of functions of bounded variation; however, most natural images do not exactly belong to this space [8]. The texture in an image plays an important role in visual quality and it is not well modeled in such a space.

Carasso in [8] formulates the image restoration problem in Lipschitz spaces where a broader class of images can be accommodated. He proposes a new approach to recover the texture in images. The central idea is the implementation of the Poisson Singular Integral (PSI), which recovers the texture where the TV fails. PSI is also utilized in [9], where its authors propose a model which combines PSI and curvelet-type decomposition space semi-norm as regularizer.

The work presented by Chen *et al.* [10] proposes the use of texture-preserving image deblurring method. The authors adopt a two-step non-iterative processing procedure which first uses regularization in the frequency domain to remove the noise, and then utilizes a modified non-local means filter to reduce the leaked colored noise in order to obtain a good texture-preserving deblurred image.

In this paper, we propose a novel algorithm for image deconvolution, using a prior model combination (TV and PSI) in order to impose different properties on the restored image. The method produces restorations with edges and textures preserved, high PSNR and good visual quality. The paper is organized as follows. In section 2, the Bayesian modeling of the problem is presented. Section 3 discusses the inference procedure and proposes an algorithm to restore the images. Section 4 contains the experimental section and, finally, section 5 concludes the paper.

## 2. BAYESIAN MODELING

The Bayesian paradigm is one of the most popular tool in image restoration (see [11] and references therein). The observation  $\mathbf{y}$  and the original image  $\mathbf{x}$  are treated as stochastic variables, and an inference process using Bayes' rule allows to obtain the restored image.

### 2.1. Observation Model

The degradation model in Eq. (1) provides the conditional probability distribution:

$$p(\mathbf{y}|\mathbf{x}, \beta) \propto \exp\left(-\frac{\beta}{2}\|\mathbf{y} - \mathbf{H}\mathbf{x}\|^2\right). \quad (2)$$

## 2.2. Image Model

In this paper we use a prior model combination, in order to ensure different properties of the restored image are presented [12]. The TV [11] prior has the advantage of preserving the edge structure while imposing smoothness on the solution. It is defined as

$$p_1(\mathbf{x}|\alpha_1) \propto \exp(-\alpha_1 \text{TV}(\mathbf{x})), \quad (3)$$

where  $\text{TV}(\mathbf{x}) = \sum_{i=1}^P \sqrt{\Delta_i^h(\mathbf{x})^2 + \Delta_i^v(\mathbf{x})^2}$  with the operators  $\Delta_i^h(\mathbf{x})$  and  $\Delta_i^v(\mathbf{x})$  corresponding to the horizontal and vertical first order differences at pixel  $i$ , respectively, and  $P$  is the image size. However, this model does not work well in textured areas. To alleviate this problem, we combine TV with the Poisson Singular Integral (PSI) [8] filter which preserves textures. The PSI filter is defined in the Fourier domain for each  $t > 0$  as

$$\mathbf{z}(\xi, \nu, t) = \left( t + \frac{4e^{-t\rho} - e^{-2t\rho} - 3}{2\rho} \right)^{1/2}, \quad (4)$$

where  $\xi, \nu$  are the coordinates in Fourier domain and  $\rho = \sqrt{\xi^2 + \nu^2}$ . We denote by  $\mathbf{Z}$  the convolution matrix associated to filter  $\mathbf{z}$  in the spatial domain, and then define the second prior model as

$$p_2(\mathbf{x}|\alpha_2) \propto \exp\left(-\frac{\alpha_2}{2} \|\mathbf{Z}\mathbf{x}\|^2\right). \quad (5)$$

Figure 1 shows a set of realizations of the PSI prior model with variance 1, for different  $t$  values. As it can be observed  $t$  controls the smoothness of the texture. As  $t$  changes so does the texture granularity (notice the log scale).

Combining both models in Eq. (3) and (5), the prior distribution is given by

$$p(\mathbf{x}|\alpha_1, \alpha_2) \propto \exp(-\alpha_1 \text{TV}(\mathbf{x}) - \frac{\alpha_2}{2} \|\mathbf{Z}\mathbf{x}\|^2). \quad (6)$$

## 3. BAYESIAN INFERENCE

The restored image sought after is the Maximum a Posteriori (MAP)

$$\begin{aligned} \hat{\mathbf{x}} &= \arg \max_{\mathbf{x}} p(\mathbf{x}|\mathbf{y}, \beta, \alpha_1, \alpha_2) \\ &= \arg \max_{\mathbf{x}} p(\mathbf{y}|\mathbf{x}, \beta) p(\mathbf{x}|\alpha_1, \alpha_2), \end{aligned} \quad (7)$$

which is obtained by minimizing

$$\mathcal{L}(\mathbf{x}) = \frac{\beta}{2} \|\mathbf{y} - \mathbf{H}\mathbf{x}\|^2 + \alpha_1 \text{TV}(\mathbf{x}) + \frac{\alpha_2}{2} \|\mathbf{Z}\mathbf{x}\|^2. \quad (8)$$

Due to use of the TV image prior, we need to utilize a majorization-minimization procedure [13]. Based on the average inequality [11], we have

$$\text{TV}(\mathbf{x}) \leq \frac{1}{2} \sum_{i=1}^P \frac{\Delta_i^h(\mathbf{x})^2 + \Delta_i^v(\mathbf{x})^2 + u_i}{\sqrt{u_i}} = \frac{1}{2} \mathbf{M}(\mathbf{x}, \mathbf{u}). \quad (9)$$

We then minimize

$$\tilde{\mathcal{L}}(\mathbf{x}) = \frac{\beta}{2} \|\mathbf{y} - \mathbf{H}\mathbf{x}\|^2 + \frac{\alpha_1}{2} \mathbf{M}(\mathbf{x}, \mathbf{u}) + \frac{\alpha_2}{2} \|\mathbf{Z}\mathbf{x}\|^2. \quad (10)$$

This procedure introduces an additional parameter set  $\mathbf{u} = (u_1, u_2, \dots, u_P)$ , calculated as (see [11] for details)

$$u_i = \Delta_i^h(\mathbf{x})^2 + \Delta_i^v(\mathbf{x})^2. \quad (11)$$

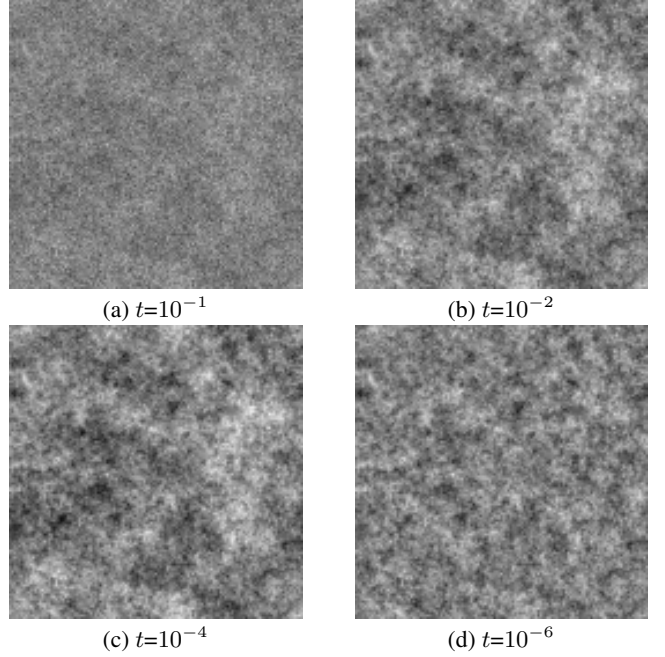


**Fig. 1.** Realizations of the prior model in Eq. (5) for different values of  $t$ .

Then the MAP estimator,  $\hat{\mathbf{x}}$ , is obtained as the solution of the linear equation system

$$\mathbf{A}\mathbf{x} = \beta \mathbf{H}^T \mathbf{y}, \quad (12)$$

where

$$\mathbf{A} = \beta \mathbf{H}^T \mathbf{H} + \alpha_1 ((\Delta^h)^T \mathbf{W} \Delta^h + (\Delta^v)^T \mathbf{W} \Delta^v) + \alpha_2 \mathbf{Z}^T \mathbf{Z}, \quad (13)$$

and  $\Delta^h$  and  $\Delta^v$  are the convolution matrices associated with horizontal and vertical gradients, respectively, and  $\mathbf{W} = \text{diag}(\frac{1}{\sqrt{u_i}})$ . We solve this system utilizing a conjugate gradient method. Since the estimation of  $\mathbf{x}$  and  $\mathbf{u}$  are coupled, we have the following iterative algorithm that alternatively estimates  $\mathbf{x}$  and  $\mathbf{u}$  until convergence.

---

### Algorithm 1 Proposed Restoration Algorithm

---

**Require:** An initial estimate of the original image,  $\mathbf{x}^0$

Set  $k = 0$

**repeat**

1. Set  $u_i^k = \Delta_i^h(\mathbf{x}^k)^2 + \Delta_i^v(\mathbf{x}^k)^2$  for  $i = 1, \dots, P$ .

2. Compute  $\mathbf{A}^k$  using the  $\{u_i^k\}_{i=1, \dots, P}$  in Eq. (13).

3. Set  $\mathbf{x}^{k+1}$  as the solution of  $\mathbf{A}^k \mathbf{x} = \beta \mathbf{H}^T \mathbf{y}$ .

4. Set  $k = k + 1$ .

**until**  $\|\mathbf{x}^k - \mathbf{x}^{k-1}\|^2 / \|\mathbf{x}^{k-1}\|^2 < \text{tol}$

---

## 4. EXPERIMENTS AND RESULTS

We tested the proposed algorithm on three different images, on three different images, *Cameraman*, *Barbara*, and *Baboon*. We chose these test images because they have different levels of spatial activity and areas with different types of texture. The images were synthetically degraded following the observation model in Eq. (2) by normalization to  $[0, 1]$  interval, blurring each original image with a

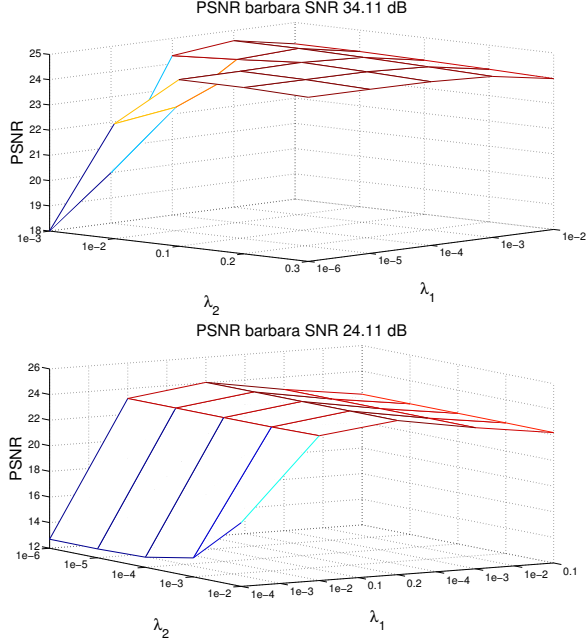


**Fig. 2.** PSNR evolution with different values of  $\lambda_1$  and  $\lambda_2$  for the *Barbara* image. (a) Degradation with a SNR of 34 dB, (b) Degradation with a SNR of 24 dB.

Gaussian blur with support  $21 \times 21$  and standard deviation 1.5. Zero mean Gaussian noise with variance  $\sigma_1^2 = 10^{-4}$  and  $\sigma_2^2 = 10^{-3}$  was added to blurred images to obtain two set of degraded images with a SNR of about 34 dB and 24 dB, respectively.

To obtain the restored images, we run Algorithm 1 starting from the degraded image as initial estimate of the original image, that is,  $\mathbf{x}^0 = \mathbf{y}$  and using  $tol = 10^{-4}$  in the stopping criterion. The proposed method depends on a set of parameters, which need to be set to obtain the best performance. The experiments have been run on an Intel(R) Core(TM) i5 2.4 GHz processor.

The PSI prior in Eq. (5) depends on the parameter  $t$  that controls the texture preservation. We run experiments to test the influence of this parameter on the restored images. We changed the parameter  $t$  in the range  $-6 \leq \log t \leq -1$ , following [8], and found that the difference on PSNR obtained with different values for the parameter  $t$  was low. This was a surprising result since the value of  $t$  conditions the shape of the prior model and it was supposed to preserve different textures on the image. Using a single value of  $t$  for the whole image is very likely not optimal and changing it locally will better adapt the algorithm to the different textures of the image. In this paper, however, we fixed  $t = 0.1$  as suggested in [8].

We searched a set of values for the parameters that control the prior and degradation models as follows. First, notice that Eq. (10) can be written as

$$\tilde{\mathcal{L}}(\mathbf{x}) = \lambda \|\mathbf{y} - \mathbf{H}\mathbf{x}\|^2 + \lambda_1 \mathbf{M}(\mathbf{x}, \mathbf{u}) + \lambda_2 \|\mathbf{Z}\mathbf{x}\|^2, \quad (14)$$

with  $\lambda = (1 - \lambda_1 - \lambda_2)$ ,

$$\lambda_1 = \frac{\alpha_1}{\beta + \alpha_1 + \alpha_2} \quad \text{and} \quad \lambda_2 = \frac{\alpha_2}{\beta + \alpha_1 + \alpha_2}. \quad (15)$$

In these equations,  $\lambda$ ,  $\lambda_1$  and  $\lambda_2$  take values in the interval  $[0, 1)$  and satisfy  $\lambda + \lambda_1 + \lambda_2 = 1$ . Thus,  $\lambda$ ,  $\lambda_1$  and  $\lambda_2$  represent the influence

**Table 1.** Numerical results for the test images.

Cameraman									
SNR=24.44 dB, PSNR=22.81 dB				SNR=34.44 dB, PSNR=23.62 dB					
Model	Param		PSNR	Time (s)	Model	Param		PSNR	Time (s)
	$\lambda_1$	$\lambda_2$				$\lambda_1$	$\lambda_2$		
TV+PSI	$10^{-2}$	$10^{-7}$	24.93	11	TV+PSI	$10^{-3}$	$10^{-7}$	<b>26.61</b>	7
TV	$10^{-2}$	0	24.93	11	TV	$10^{-3}$	0	<b>26.61</b>	7
PSI	0	$10^{-1}$	24.20	1	PSI	0	$10^{-2}$	25.90	1
LOG			<b>25.26</b>	13	LOG			26.25	11

Barbara									
SNR=24.11 dB, PSNR=23.01 dB				SNR=34.11 dB, PSNR=23.88 dB					
Model	Param		PSNR	Time (s)	Model	Param		PSNR	Time (s)
	$\lambda_1$	$\lambda_2$				$\lambda_1$	$\lambda_2$		
TV+PSI	$10^{-2}$	$10^{-4}$	24.03	45	TV+PSI	$10^{-4}$	$10^{-1}$	<b>24.65</b>	4
TV	$10^{-2}$	0	24.03	41	TV	$10^{-3}$	0	24.59	12
PSI	0	$10^{-1}$	23.88	2	PSI	0	$10^{-2}$	24.60	4
LOG			<b>24.09</b>	44	LOG			24.42	41

Baboon									
SNR=24.56 dB, PSNR=21.25 dB				SNR=34.56 dB, PSNR=21.80 dB					
Model	Param		PSNR	Time (s)	Model	Param		PSNR	Time (s)
	$\lambda_1$	$\lambda_2$				$\lambda_1$	$\lambda_2$		
TV+PSI	$10^{-3}$	0.2	<b>22.27</b>	12	TV+PSI	$10^{-7}$	$10^{-1}$	<b>23.33</b>	2
TV	$10^{-3}$	0	21.88	29	TV	$10^{-4}$	0	23.11	8
PSI	0	$10^{-1}$	22.02	2	PSI	0	$10^{-2}$	23.33	4
LOG			22.10	43	LOG			23.21	32

on the restored image of the observed data, the TV, and the PSI models, respectively. Notice that selecting  $\lambda_1$  and  $\lambda_2$  in Eq. (14) is easier and more intuitive than selecting  $\beta$ ,  $\alpha_1$  and  $\alpha_2$  in Eq. (10). We performed a search on this range by moving  $\lambda_1$  and  $\lambda_2$  in the set of values  $[0, 10^{-7}, 10^{-6}, 10^{-5}, 10^{-4}, 10^{-3}, 10^{-2}, 0.1, 0.2, 0.3, 0.4]$ , and as we indicated above setting  $\lambda$  to  $1 - \lambda_1 - \lambda_2$ . We note that for values of  $\lambda_1$  or  $\lambda_2$  larger than 0.4 the quality of the restored image reduces drastically so we did not consider them in our experiments. In Fig. 2 we present the evolution of the PSNR as a function of  $\lambda_1$  and  $\lambda_2$  for the *Barbara* image for the two noise degradations considered. In both cases, the shape of the curve is similar. We note that the value of the PSNR is quite similar around this maximum, which means that the method is not very sensitive to different values of the parameters  $\lambda_1$  and  $\lambda_2$ . This behavior was also observed on the rest of the test images so it confirms that it is not needed to select the parameters with a high precision to obtain good restorations.

However, we found significant differences on the values of the parameters that achieve the maximum PSNR for the different images. The values of the parameters, the computational time and the value of the PSNR for the observed and restored images are summarized in Table 1. This table also includes, for comparison purposes, the figures of merit for the recently proposed log prior model in [3] (LOG). Although, the method in [3] was formulated as a blind deconvolution method, in this paper, we assume that the blur and the noise variance are known. We can extract some conclusions from those values. First, as the noise increases, higher reliance on prior information is needed and, hence, the values of the parameters  $\lambda_1$  and  $\lambda_2$  increase. Second, the relation of the importance of the PSI and TV models highly depend on the contents of the image. So, if the image presents a low level of detail, as it happens in the *cameraman* image, the restoration method prefers smooth restorations and the maximum value for the PSNR is obtained when  $\lambda_2$  is equal to zero, giving control of the smoothness of the solution to the TV prior model. If the image also presents high level of noise, slightly better results are obtained by the LOG method, because it better controls the high noise. However, if the image contains a very high level of detail, as is the case with the *Baboon* image, better results are obtained if the TV prior influence is almost neglected by setting the



Fig. 3. Original *Barbara* image.

value of  $\lambda_1$  very close to zero and leaving the control of the noise and texture preservation to the PSI prior model. This is expected since the TV prior tends to smooth out the small details in the image. Note however that, as the noise increases, including a small contribution by the TV prior provides better results since the PSI prior cannot differentiate between highly detailed textures and noise [9]. In images with a combination of detailed and smooth regions, a combination of both prior models provides the best result for the proposed method. This is the case with the *Barbara* image that reaches its maximum PSNR when  $\lambda_1$  and  $\lambda_2$  are both greater than zero.

For visual evaluation of the results, Fig. 3 shows the original *Barbara* image and Fig. 4 shows the observed images for different noise levels, the restorations with the proposed method using different values for the parameters  $\lambda_1$  and  $\lambda_2$ , and the restoration with the LOG method. Although all restored images present a high quality, the image obtained using a combination of the TV and the PSI models (Figs. 4i and 4j) show a higher visual quality and better preserve textures in areas as the handkerchief and the tablecloth while controlling noise, as can be seen in the details in Fig. 5. The image obtained using only the TV prior, that is, using  $\lambda_2 = 0$  (Figs. 4e and 4f) and the LOG method (Figs. 4g and 4h) look flat and most of the texture has been lost while the images using only the PSI prior ( $\lambda_1 = 0$ ), depicted in Figs. 4c and 4d, are noisy. This agrees with the numerical results in Table 1. Notice that when the noise is higher, more contribution of the TV prior was needed in order to eliminate noise and, thus, texture in the restored image, as the handkerchief and the trousers, could not be successfully recovered.

## 5. CONCLUSIONS

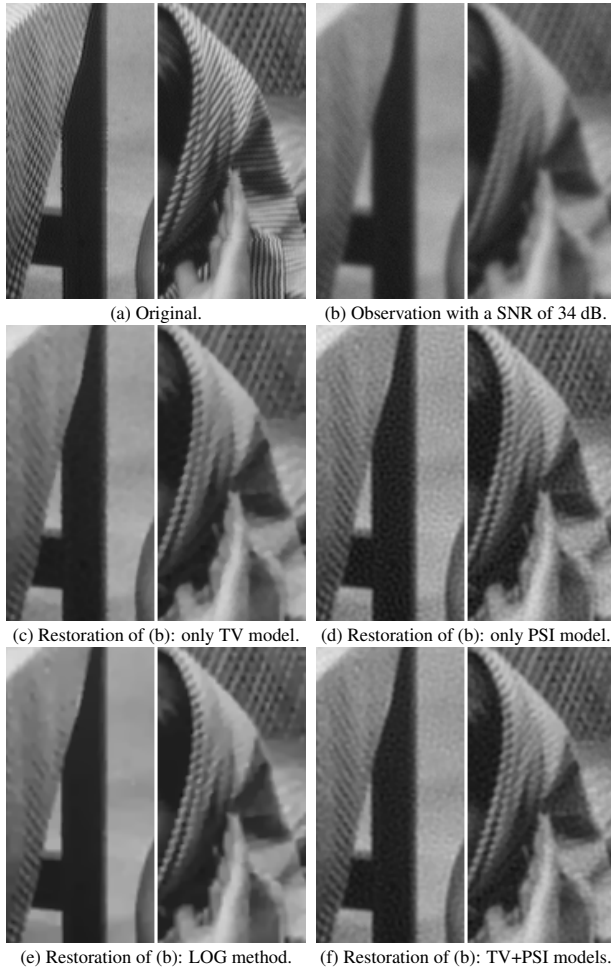
In this paper we present a novel methodology to restore blurred images with noise. The combination of TV and PSI prior models provides better visual quality and PSNR than utilizing both models alone. The model recovers fine-scale details (texture) in cases where TV completely fails and our experimental results confirm this. The proposed method shows good performance on images with a combination of detailed and smooth regions, and textured images with high noise where the combination of TV and PSI controls the noise while preserving the details. The proposed method depends on a series of parameters whose value needs to be fixed or estimated from the available data. Although in this paper those parameters are selected to obtain the best results, in future works, we aim to automatically estimate the parameters together with the restored image.



Fig. 4. Experimental results for the *Barbara* image.

## 6. REFERENCES

- [1] J.-L. Stark, F. Murtagh, and J. M. Fadili, *Sparse image and signal processing*, Cambridge University, 2010.
- [2] E. Shaked and O. V. Michailovich, “Deconvolution of Poissonian images via iterative shrinkage,” *IEEE International Symposium on Biomedical Imaging: From Nano to Macro (ISBI)*, pp. 1309–1312, April 2010.
- [3] S. D. Babacan, R. Molina, M. N. Do, and A. K. Katsaggelos, “Blind deconvolution with general sparse image priors,” in *European Conference on Computer Vision (ECCV)*, September 2012, pp. 341–355.
- [4] M. Tallón, J. Mateos, S. D. Babacan, R. Molina, and A. K. Katsaggelos, “Space-variant kernel deconvolution and denoising in dual exposure problem,” *Information Fusion*, vol. 14, no. 4, pp. 396–409, October 2013.
- [5] M. Hirsch, C. J. Schuler, S. Harmeling, and B. Scholkopf, “Fast removal of non-uniform camera shake,” in *International Conference on Computer Vision (ICCV)*, November 2011, pp. 463–470.
- [6] S. D. Babacan, R. Ansorge, M. Luessi, P. Ruiz, R. Molina, and A. K. Katsaggelos, “Compressive light field sensing,” *IEEE Transactions on Image Processing*, vol. 21, no. 12, pp. 4746–4757, December 2012.
- [7] L. I. Rudin, S. Osher, and E. Fatemi, “Nonlinear total variation based noise removal algorithms,” *Physica D*, pp. 259–268, November 1992.
- [8] A. S. Carasso, “Singular integrals, image smoothness, and the recovery of texture in image deblurring,” *SIAM Journal on Applied Mathematics*, vol. 64, no. 5, pp. 1749–1774, June–July 2004.
- [9] L. Huang, L. Xiao, Z. Wei, and Z. Zhang, “Variational image restoration based on Poisson singular integral and curvelet-type decomposition space regularization,” in *IEEE International Conference on Image Processing (ICIP)*, September 2011, pp. 685–688.
- [10] F. Chen, X. Huang, and W. Chen, “Texture-preserving image deblurring,” *IEEE Signal Processing Letters*, vol. 17, no. 12, pp. 1018–1021, December 2010.
- [11] S. D. Babacan, R. Molina, and A. K. Katsaggelos, “Variational Bayesian blind deconvolution using a total variation prior,” *IEEE Transactions on Image Processing*, vol. 18, no. 1, pp. 12–26, January 2009.
- [12] M. Vega, J. Mateos, R. Molina, and A. K. Katsaggelos, “Astronomical image restoration using variational methods and model combination,” *Statistical Methodology*, vol. 9, no. 1-2, pp. 19–31, January 2012.
- [13] S. D. Babacan, R. Molina, and A. K. Katsaggelos, “Parameter estimation in TV image restoration using variational distribution approximation,” *IEEE Transactions on Image Processing*, vol. 17, no. 3, pp. 326–339, March 2008.



**Fig. 5.** Details of the restorations in Fig. 4.